Biosensors and Bioelectronics 271 (2025) 117098

Contents lists available at ScienceDirect

Biosensors and Bioelectronics

journal homepage: www.elsevier.com/locate/bios

Dual-compartment-gate organic transistors for monitoring biogenic amines from food

Ilenia Sergi [a,b], Matteo Sensi [a,*], Rian Zanotti [c], Theofania Tsironi [d], Emmanouil Flemetakis [e], Deborah Mary Power [f], Carlo Augusto Bortolotti [a], Fabio Biscarini [a,g]

[a] Department of Life Sciences, Università Degli Studi di Modena e Reggio Emilia, Via Campi 103, Modena, 41125, Italy
[b] Department of Neurosciences and Rehabilitation, Università Degli Studi di Ferrara, Via Fossato di Mortara 17/19, Ferrara, 44121, Italy
[c] Department of Physics, Informatics and Mathematics, Università Degli Studi di Modena e Reggio Emilia, Via Campi 213/a, Modena, 41125, Italy
[d] Department of Food Science and Human Nutrition, Agricultural University of Athens, Athens, 11855, Greece
[e] Department of Biotechnology, Agricultural University of Athens, Athens, 11855, Greece
[f] Centro de Ciencias Do Mar, Universidade Do Algarve, Campus de Gambelas, 8000-117, Faro, Portugal
[g] Center for Translational Neurophysiology of Speech and Communication, Istituto Italiano di Tecnologia (CTNSC), Via Fossato di Mortara 17-19, Ferrara, 44121, Italy

A B S T R A C T

According to the Food and Agriculture Organization of the United Nations (FAO) more than 14% of the world's food production is lost every year before reaching retail, and another 17% is lost during the retail stage. The use of the expiration date as the main estimator of the life-end of food products creates unjustified food waste. Sensors capable of quantifying the effective food freshness and quality could substantially reduce food waste and enable more effective management of the food chain. We propose an electrolyte-gated organic transistor (EGOT) that responds to the release of biogenic amines, like diamines and tyramine, generated by the degradation of protein-rich food. The EGOT sensor features a polymeric poly(3,4-ethylenedioxythiophene) polystyrene sulfonate (PEDOT:PSS) gate electrode fabricated in the shape of a miniaturized beaker containing an aqueous solution in the inner side (to be exposed to food) and capacitively coupled through a hydrogel to the transistor channel on the outside (not in contact with food). The hydrogen bonds formed by the water-dissolved amines with PEDOT:PSS modulate the EGOT channel across a wide range of amine concentrations. We demonstrate that our sensor can detect different amines by the combinatorial analysis of the response from different channel materials, PEDOT:PSS and the other DPP-DTT, with a limit of detection as low as 100 pM.

1. Introduction

As the human population grows, food freshness and safety become crucial both to feed the increasing human population and to prevent risks to consumer health. Over 200 diseases are caused by eating food contaminated with bacteria, viruses, parasites, or chemicals, and it is essential to ensure that consumed food is not contaminated or that an unacceptable loss in freshness and quality occurs across the entire food chain. Contamination can occur in various stages of food processing, such as during production, preparation, packaging, distribution, and consumption (Nerín et al., 2016). Food poisoning can be caused by parasites, viruses, bacteria, and chemical or natural toxins, such as aflatoxins, and mycotoxins, but also from molecules generated by food spoilage like biogenic amines (BAs) (Ruiz-Capillas and Herrero, 2019) or volatile organic compounds (VOCs). BAs can cause neurotransmission disorders, such as nausea, headaches, and palpitations, especially when ingested with monoamine oxidase inhibitors, like drugs or alcohol (Omer et al., 2021).

BAs are low molecular weight aliphatic, heterocyclic, or alicyclic bases that are primarily biosynthesized in plants, animals, and microorganisms. The most relevant BAs (Bachrach. U, 2005) related to food spoilage are histamine (His), tyramine (Tyr), tryptamine (Try), thiourea (Thi), dopamine (DA), N-butylamine (NBA), o-phenylenediamine (OPD), 2-aminopyridine (2-AP), ethylenediamine (EDA), aniline (Ani), cadaverine (Cad) and putrescine (Put). BAs are biochemical indicators of food safety and quality, often used as a freshness index in fish and shellfish products (Doeun et al., 2017). They are categorized into endogenous and exogenous BAs, with endogenous BAs being synthesized in an organism's tissues and exogenous BAs being absorbed directly from food in the intestine. BAs are produced through the amination or transamination of ketones and aldehydes, or by decarboxylation of amino acid precursors(Wang et al., 2019). The FAO/WHO expert meeting on the public health risks of histamine and other BAs has reported BA thresholds in fish species. Ingestion of BAs may be more adverse in sensitive consumers with reduced mono and diamine oxidase activity (Li and Lu, 2020). Prevention strategies for BAs poisoning

* Corresponding author.
E-mail address: matteo.sensi@unimore.it (M. Sensi).

https://doi.org/10.1016/j.bios.2024.117098
Received 28 June 2024; Received in revised form 11 December 2024; Accepted 22 December 2024
Available online 23 December 2024

include good manufacturing practices, high-quality components, temperature control, amine oxidants, high hydrostatic pressure, decreasing amine residues and free amino acids, using amine-negative starter cultures, and inhibiting amine-positive bacterial strain growth (Doeun et al., 2017).

Evaluating BAs levels is directly linked to their effect on food product quality and detecting trace levels in a complex food matrix is a major challenge (Verma et al., 2020; Torre et al., 2020; Arulkumar et al., 2023; Biji et al., 2016). Detecting BAs in foods using chromatographic techniques like capillary electrophoresis, gas chromatography, TLC, and HPLC is essential, but these methods have disadvantages such as expensive equipment, specialized personnel, and time-consuming pretreatment and derivatization of complex samples (Önal, 2007). At the market level, no biosensors are available for the quantification of single biogenic amines. BAs concentrations can greatly change in different food sources, from the nM to mM. In the literature we can find mostly electrochemical biosensors based on MAO (Vasconcelos et al., 2021), gold nanoparticles (Li et al., 2021), or MIPs (Givanoudi et al., 2023), with the lowest observed limit of detection (LOD) of 40 nM for tyramine. Chemosensors may be a simple, fast, robust, and cost-effective alternative to current approaches for the detection of BAs (Erim, 2013). In the past decade, electrolyte-gated organic transistors (EGOTs) emerged as sensitive label-free immunosensors (Berto et al., 2018; Sensi et al., 2021, 2023) and enzymatic sensors (Magliulo et al., 2016). EGOT sensors are characterized by a transistor architecture, consisting of two interdigitated source (S) and drain (D) electrodes bridged by an organic semiconductor channel that is also in contact with the gate electrode (G) through an electrolyte. Thanks to the capacitive coupling between the gate/electrolyte and electrolyte/channel interfaces, any recognition event taking place on the gate or the channel, is amplified by the organic semiconductor and is measurable in terms of change in the output current (Burtscher et al., 2021). The selectivity of the EGOT sensor is achieved by functionalization of one of the two interfaces with a recognition moiety, like antibodies, aptamers, oligonucleotides, or polymers (Torricelli et al., 2021) able to selectively interact with the target analyte.

The most sensitive and widely explored EGOT sensors have a functionalized gate electrode for target recognition (Casalini et al., 2015). The usefulness of EGOT sensors has mainly been demonstrated for bio-medical targets, such as oligonucleotides (Kergoat et al., 2012; Sensi et al., 2022), proteins (Berto et al., 2016; Gentili et al., 2018; Guo et al., 2021; Pappa et al., 2018), neurotransmitters (Gualandi et al., 2016), antibodies (Sensi et al., 2024), and cells (Song et al., 2023; Strakosas et al., 2015).These devices are even capable of single-molecule detection (Macchia et al., 2018). Relatively few examples exist exploring the potential of EGOTs for the detection of food targets (Bihar et al., 2016; Gentile et al., 2022; Gualandi et al., 2020) and have mainly focused on amines (Minami et al., 2015; Minamiki et al., 2018). In most EGOT sensors both the electrode gate and semiconductor channel are in contact with the aqueous electrolyte which may result in exchange, transport, and cross-contamination of channel and gate with the analytical target or similar molecules, thus introducing non-specific contributions to the signal. For these reasons more complex architectures were proposed with two distinct electrolyte compartments where the recognition occurs at a floating gate separated from the extended gate driving the channel (Lai et al., 2018; White et al., 2016).

Here we propose an innovative EGOT architecture where there is no floating gate for recognition, instead, the extended gate itself compartmentalizes the recognition events and the channel gating in two separate regions, one for recognition and one for transduction. The innovation associated with the gate electrode is that the functions of the extended and floating gate are both encompassed by a monolithically moulded conductive polymer (PEDOT:PSS) hydrogel (Arthur et al., 2022) shaped as a small beaker. This device can be easily fabricated with simple processes. We demonstrate that our device enables the selective recognition of biogenic amines thus revealing its potential as a food freshness indicator, with a theoretical LOD at the state of the art for this application.

2. Results and discussion

2.1. Fabrication of the dual-compartment gate electrode

The process to fabricate the miniaturized beaker gate is shown in Fig. 1a. The gate electrode is fabricated by casting and thermal curing of a PEDOT:PSS solution enriched in DMSO inside a polypropylene cup used as the mould. The capillary forces pin the meniscus to the vertical wall of the cup, thus keeping the wall wet. As a consequence, the PEDOT:PSS gate acquires the inner shape of the cup rather than forming a disk.

We use the PEDOT:PSS gate as a dual-compartment hydrogel electrode that effectively integrates the functions of an extended gate-floating gate in compartmentalized EGOT sensing architectures: on one side (separated from the channel) a drop of aqueous solution is placed to adsorb the biogenic amines, on the other side the gate is coupled to the polymer thin film channel through a solid electrolyte (agar). We use either PEDOT:PSS (Galliani et al., 2020; Rivnay et al., 2018; Kumar et al., 2015); or Poly [2,5-(2-octyldodecyl)-3,6-diketopyrrolopyrrole-alt-5,5-(2,5-di(thien-2-yl)thieno [3,2-b]thiophene)], DPP-DTT (Jia et al., 2021; Pallu et al., 2019; Chennit et al., 2023), thin films as channels. Both materials are p-type semiconductors, but while PEDOT:PSS is a mixture of two ionomers working in depletion mode, DPP-DTT is an organic donor-acceptor polymer, working in accumulation mode. The polymeric films are drop-cast on interdigitated electrodes from water dispersions for PEDOT:PSS and spin-cast from 1, 2-dichlorobenzene solutions for DPP-DTT and cured in oven for 30 min at 120 °C and 140 °C respectively.

2.2. Electrical characterization of EGOTs with dual-compartment hydrogel gate electrode

Our idea behind the EGOT sensor for biogenic amines stems from the weak bonds established between PEDOT:PSS and charged amines (Giordani et al., 2020; Hsieh et al., 2021; Jing et al., 2023; Keene et al., 2020; Marutaphan et al., 2017; Van Der Pol et al., 2019). The large-area dual-compartment hydrogel gate maximizes the bonds and amplifies the binding process, avoiding the interactions between the amines and the channel. In the experimental procedure, the analyte solution is introduced inside the PEDOT:PSS hydrogel gate of the EGOT, while the connection between the gate and the semiconductive channel is achieved through an agar hydrogel electrolyte, touching the other side of the gate.

Fig. 1c shows a schematic representation of the EGOT configuration, where the channel, is made either of PEDOT:PSS or DPP-DTT. The difference between these two p-type materials is in the polarization applied to the gate electrode (in Fig. 1c the DPP-DTT transistor is depicted), viz. positive gate bias for PEDOT:PSS, negative for DPP-DTT. The operation of the devices with the hydrogel gate and electrolyte was assessed by measuring transfer curves (Fig. 1d–e). The voltage between the Source (S) and the Drain (D) electrodes (V_{DS}) was fixed at −0.1 V, to operate the device in linear regime, and the current variation in the channel (I_{DS}, namely the current in the semiconductive channel) was measured as a function of the potential difference applied between G and S (V_{GS}). V_{GS} was swept between −0.2 V and 0.6 V for the PEDOT:PSS-based EGOT (Fig. 1d), which works in depletion mode, and between −0.1 V and −0.7 V for the DPP-DTT based device (Fig. 1e), which is operated in accumulation regime.

We extract the transconductance (g_m) as the first derivative of the transfer curve (Fig. 1e and d), which is a useful property to evaluate the ability of the device to amplify a small voltage variation in a large current difference and how this is affected by the sensing process. The data show a maximum transconductance in both devices at 0.1 V for the PEDOT:PSS, and −0.6 V for DPP-DTT. Both configurations exhibit

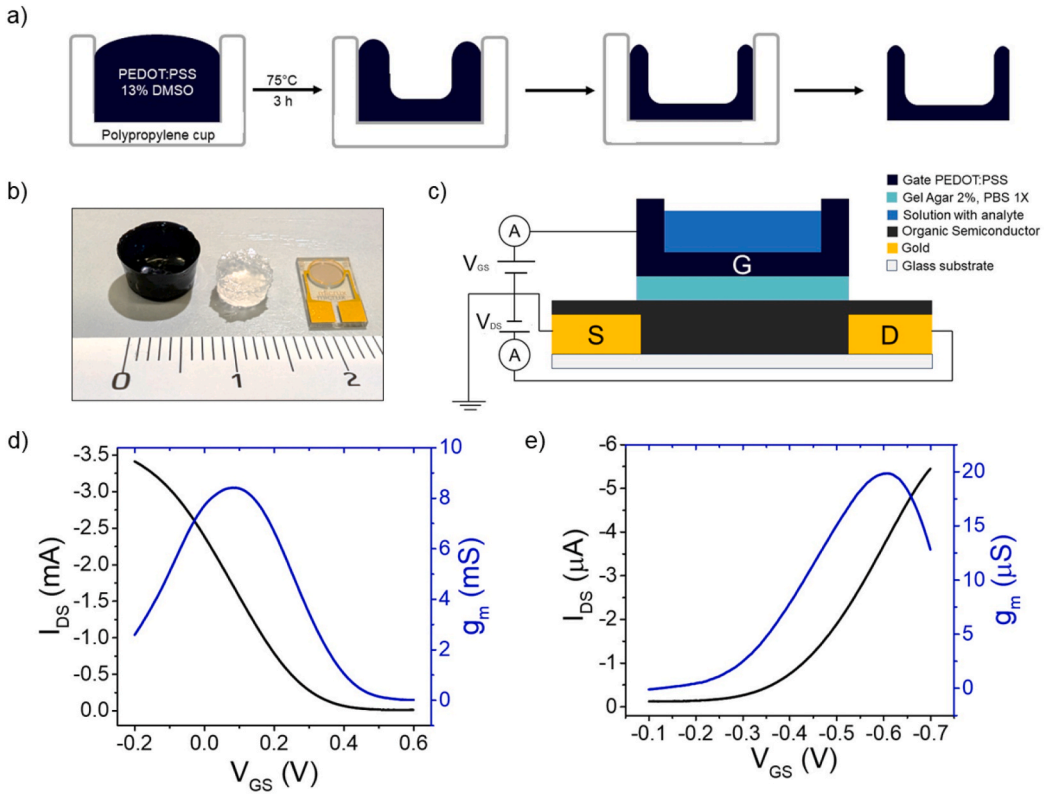

Fig. 1. Gate fabrication and EGOT architecture. a) Fabrication process b) Device components, from the left to the right: interdigitated electrodes, solid electrolyte (agar), PEDOT:PSS hydrogel beaker. c) Schematic drawing of the experimental setup with electrical connections (the ones shown refer to the DPP-DTT EGOT). d, e) Transfer characteristics of the EGOTs and correlated transconductance (respectively device based on PEDOT:PSS and DPP-DTT).

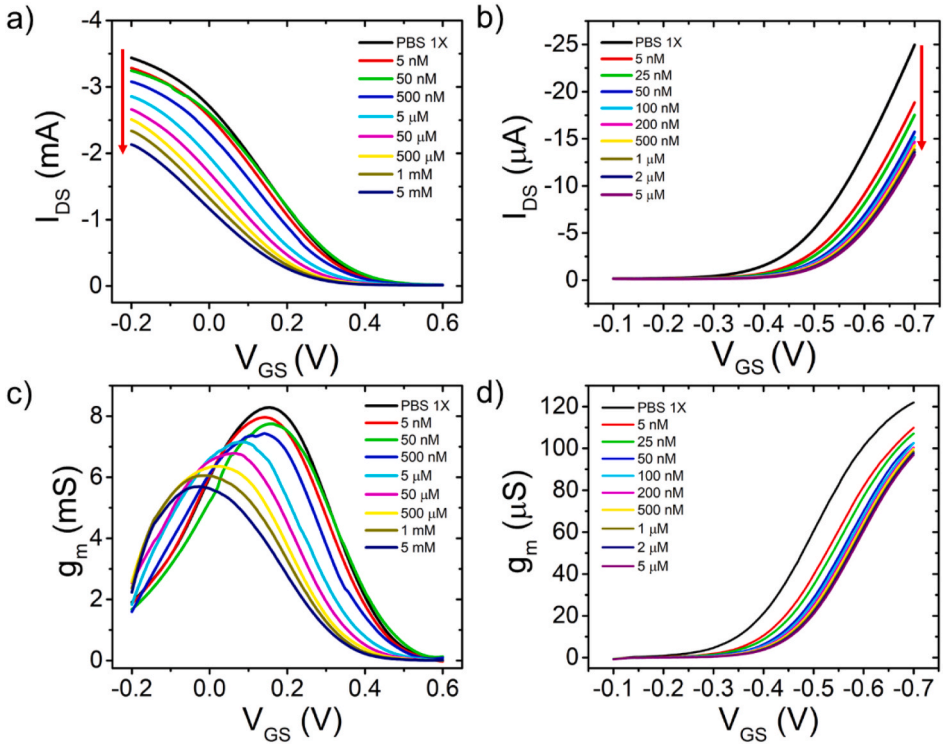

Fig. 2. Tyramine sensing a, b) Transfer characteristics of EGOTs for PEDOT:PSS and DPP-DTT based devices respectively, upon exposure to different Tyramine solutions in PBS (Tyramine concentrations are reported in the legend). $V_{DS} = -0.1$ V c, d) Transconductance of EGOTs (PEDOT:PSS and DPP-DTT based devices respectively). The I_{GS} measured during the sensing are reported in Fig. S1 of Appendix A.

excellent performance in terms of current, g_m and voltage range of operation compared to devices with the same channel materials in the literature.

2.3. Biogenic amines sensing

The device response toward Tyramine was monitored by recording the transfer curves in the presence of different concentrations of the analyte to build a standard dose-response curve. The device was first tested with a 1X PBS solution as the blank and then with increasing known concentrations of the analyte diluted in the same buffer. We measured a range of concentrations spanning between 5 nm and 5 mM (Fig. 2a and b). For both the devices we observed a monotonic I_{DS} decrease as the [Tyramine] concentration increased. From the trend of the slope in the linear region of the transfer curves (between ~ −0.1 V and ~0.2 V and < −0.6 V for PEDOT:PSS-based and DPP-DTT-based devices respectively) we observe a monotonic decrease as a function of the analyte concentration. The results obtained suggest that at the gate, the amine which is positively charged at pH 7.4 in the PBS buffer binds PEDOT:PSS through hydrogen bonds. This interaction will make the PEDOT:PSS potential at the gate more positive/less negative. Then, the gate electrode will push more cations/less anions towards the channel. Either occurrence will decrease the hole carrier density in the PEDOT:PSS channel or the DPP-DTT channel, hence the I_{DS} current will decrease upon increasing concentration of the biogenic amine and the signal will become more negative. In the measurements performed with PEDOT:PSS channels, so with positive gate potential, we cannot exclude oxidation of tyramine at high concentrations and partial electrodeposition of polytyramine, as shown by the peak at 0.5 V that appears in the I_{GS} currents (Fig. S1 in Appendix A) when [TYR] > 500 μM.

EGOTs are multiparametric devices, which means that the bio-recognition event at the gate can be monitored by various figures of merit, like threshold voltage (V_{th}) and g_m (Fig. 2c and d). Transconductance in EGOTs is defined as the product of the charge carriers' mobility (μ), effective capacitance C_{eff}, $V_{DS,}$ and the weight/length ratio of the channel (W/L). In this work, we monitored the sensing process by taking into account the signal of the current at a specific V_{GS}:

$$S = \frac{I_{DS,[BA]} - I_{DS,0}}{I_{DS,0}} \quad \text{eq. 1}$$

Where $I_{DS,[BA]}$ is the current measured in the presence of a specific biogenic amine concentration and $I_{DS,0}$ is the current measured with only PBS inside the gate electrode, both at the same V_{GS}.

As shown in Fig. 2a and b, upon exposure to tyramine, we observe a monotonic decrease of both the current and transconductance in the devices with PEDOT:PSS and DPP-DTT channels.

A different range of concentrations of [Tyramine] was used with the two channels because devices with DPP-DTT saturates (i.e. the curves following [Tyramine] = 1 μM are superimposed) at lower concentrations compared to PEDOT:PSS based EGOTs. The maximum g_m of the device based on PEDOT:PSS (Fig. 2c) decreases from 8 mS to 5.5 mS as a function of [Tyramine]. For the device based on DPP-DTT, the maximum g_m decreases when [Tyramine] increases from 120 to 100 μS.

The dose curves S vs [Tyramine] at V_{GS} = 0.4 V and 0.2 V for PEDOT:PSS devices and −0.2 and −0.5 V for DPP-DTT devices, are shown in Fig. 3a and b. The interaction between Tyramine and the hydrogel gate induces a decrease of signal for both channel materials and shows that PEDOT-PSS sensors can be operated at higher Tyramine concentrations while DPP-DTT sensors are saturated at micromolar Tyramine levels. Nevertheless, despite this limitation, it is relevant that the DPP-DTT sensors can detect lower concentrations compared to PEDOT:PSS ones,

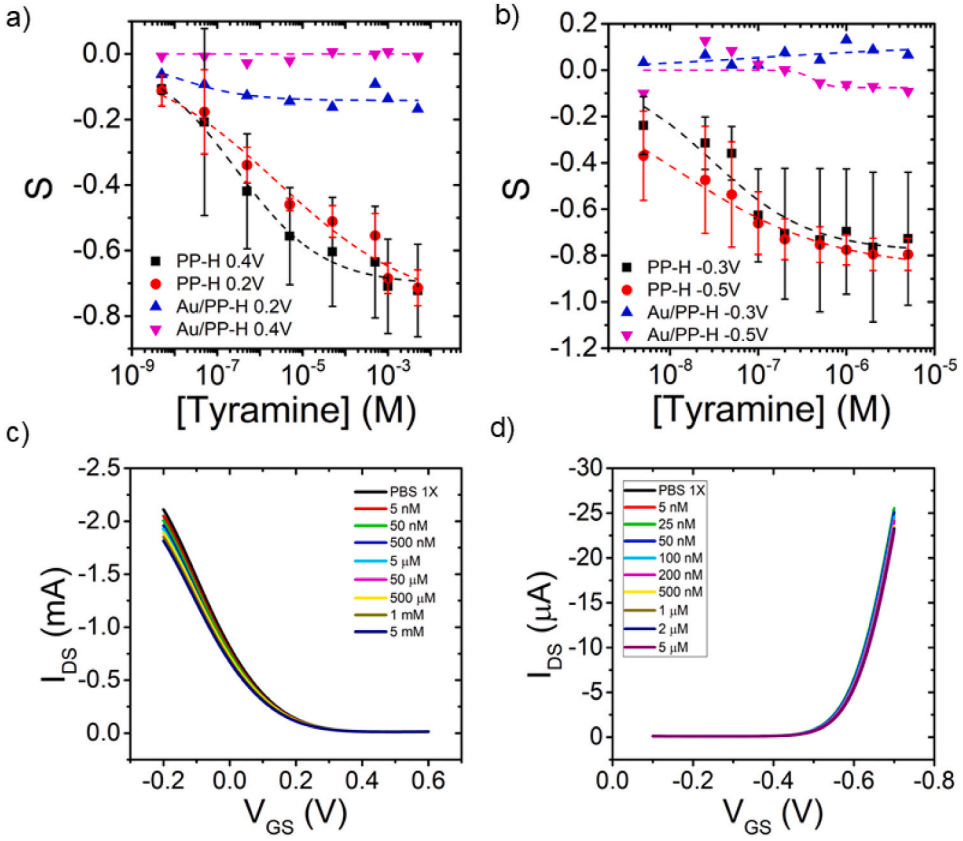

Fig. 3. Control experiment. a, b) Dose curve S versus [Tyramine] acquired at V_{GS} = 0.2 V, 0.4 V and at V_{GS} = −0.3 V, −0.5 V using an untreated gate and the gate covered by Au-NPs. Device based on (a) PEDOT:PSS and (b) DPP-DTT; c, d) Transfer characteristics of EGOTs based on (c) PEDOT:PSS and (d) DPP-DTT, resulting from exposure to different [Tyramine] solutions in PBS using the gate covered by Au-NPs.

with a theoretical LOD of around 100 pM (calculated as described in the experimental section).

Since the channel materials are not directly involved in the sensing process but mainly in the transduction of the gate potential changes at the electrode, we infer that the different behaviour is due to the electrostatic interactions between the amines and the gate induced by the applied V_{GS}, which is positive for PEDOT:PSS and negative for DPP-DTT. The negative V_{GS} applied on the gate in DPP-DTT devices could even be attractive for the positively charged amines, promoting the formation of PEDOT: PSS/amine bonds on the gate. In devices with PEDOT:PSS channel, instead, higher concentrations of Tyramine are resolved, because the positive V_{GS} applied on the gate induces a slight repulsion between the positively charged amines and the gate itself.

The signal of the device based on PEDOT:PSS shows a rapid decrease at low concentrations (under 5 μM) followed by a plateau at high concentrations. A similar trend is observed in the device based on DPP-DTT where the plateau starts at lower concentrations (200 nM).

As a confirmation of the nature of the bonds formed between the gate and the analyte, we performed a control experiment covering the gate side exposed to the analyte with electroplated gold nanoparticles (Au-NPs). This procedure aims to hinder the interaction between PEDOT:PSS and amines by covering the PEDOT:PSS with a gold layer. The absence of response to tyramine in both device configurations, reported in Fig. 3, demonstrates that the deposited gold prevents the formation of bonds between tyramine and the gate, thus confirming our suggested working principle for the fabricated device.

In food samples we expect the presence of various biogenic amines; for this reason, we tested the device response in the presence of a diamine, introducing in the gate increasing concentrations of Ethylenediamine (EDA, in the same concentration range as used for Tyramine).

In Figs. 4a and 5a we report the dose curves obtained by extracting the signals from three sets of transfer curves for each channel material. For both the devices, I_{DS} decreased as the [EDA] increased and the corresponding dose curves, extrapolated by calculating the signal at $V_{GS} = 0.2$ V (for devices based on PEDOT:PSS, Fig. 4a) and $V_{GS} = -0.5$ V (for devices based on DPP-DTT, Fig. 5a), were compared to the results obtained with Tyramine. From the comparison, we observe that although the signal values are similar for EDA and Tyramine when the signal of the current is fitted with a Hill isotherm just to guide the eye of the reader (dashed curves in Fig. 4, details on of the fit are discussed in Appendix A, section 4), these chemicals present distinguishable trends. As a control, we verified the response of the device to another charged analyte (Malic Acid, negatively charged at pH 7.4), which showed a clearly lower response compared to the amines (Appendix A, Fig. S3).

To obtain a deeper description of the response of the devices, in terms of influence of the analyte on the channel material, we fitted the transfer curves with a new EGOT analytical model that we recently published (Zanotti et al., 2024). The fitting of the transfer curves with equation 18 in the cited paper provides four parameters that we can monitor as a function of the analytes and the channel materials: V_t (switch-on voltage), $g_{m,l}$ (linear transconductance), α (ratio of the areal charge densities), and σ (energy disorder). The V_T represents the gate voltage at which the (semi)conductor is in the flatband or charge neutrality condition. Like the commonly used threshold voltage, V_T depends on work function variations of the gate electrode, or of the semiconductive channel. The determination of V_T does not require a previous assumption of the regime (i.e. linear or saturation) where the measurements are conducted, which is an important advantage compared to threshold voltage. For highly doped organic semiconductors, like PEDOT:PSS α is directly correlated to volumetric capacitance, as discussed in Zanotti et al., (2024). The fitting procedure also requires fixing the minimum current, defined as the lower current measured in each transfer curve, in the order of 10–100 nA for DPP-DTT devices and few μA for PEDOT:PSS devices, and the band gap of the channel material, 1.7 eV for both materials (Zanotti et al., 2024). As

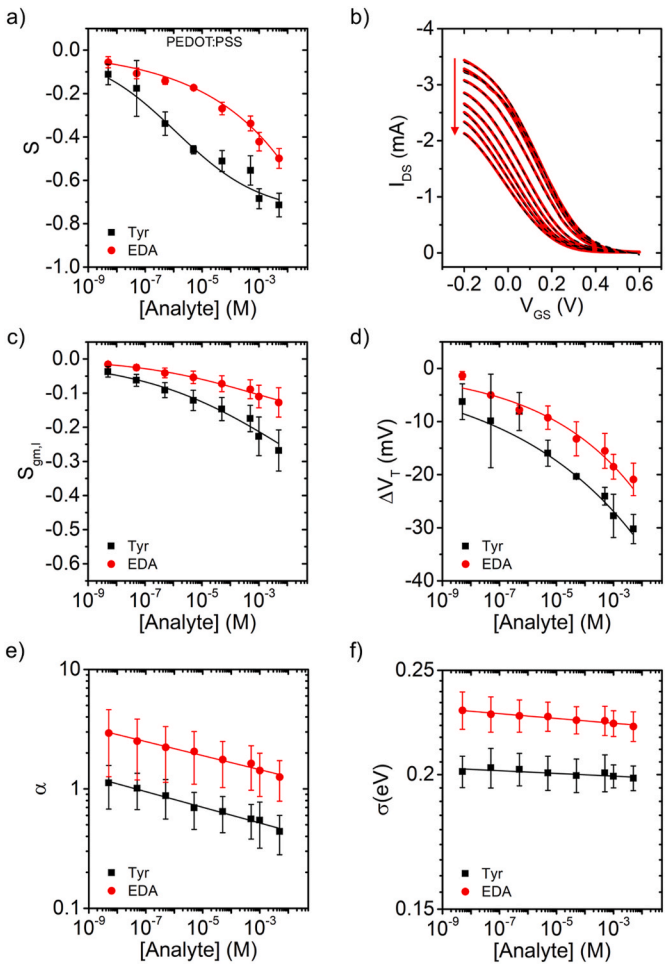

Fig. 4. Analysis of the response of PEDOT:PSS devices. a) Signal of the current of PEDOT:PSS devices as a function of biogenic amines concentration. The lines are a guide for the eye of the reader. b) Dashed lines are the best fit curves obtained using eq 18 in (Zanotti et al., 2024) of the transfer curves reported in Fig. 2a. Best fit parameters as a function of amines concentration: c) transconductance signal $S_{gm,l}$, d) switch-on voltage shift ΔV_t, e) α and f) energy disorder σ.

shown by the dashed lines in panel b of Figs. 4 and 5, the best fit precisely accurately reproduces the whole transfer curves of the devices with either PEDOT:PSS or DPP-DTT channels. The signal of the linear transconductance $S_{gm,l} = (g_{m,l} - g_{m,l0})/g_{m,l0}$ shows a decreasing monotonic trend for PEDOT:PSS EGOTs, reaching a minimum of −13% for EDA and −27% for Tyramine at the highest concentration (Fig. 4c). A similar trend can be observed also for the $\Delta V_t = V_t - V_{t,0}$ plot in Fig. 4d, where $V_{t,0}$ is the V_t measured without the target analyte. ΔV_t decreases monotonically as a function of EDA and tyramine, reaching a minimum of −20 mV and −30 mV respectively at the highest concentration. The α parameter, related to the charge carriers and the capacitance of the double layer, is also affected by the analyte concentration, decreasing with both amines (Fig. 4e). The energy disorder parameter σ is not affected by the analyte concentration, suggesting that the channel is not directly modified and does not interact with the analyte, as expected (Fig. 4f). In all the plots the variation induced by EDA is always lower compared to the one induced by tyramine, suggesting the possibility in the future to maximize this difference to selectively evaluate the single amines.

The $S_{gm,l}$ obtained from the fitting of the DPP-DTT transfer curves, shown in Fig. 5c, decreases as a function of EDA (−35% at 5 μM) and tyramine (−39% at at 5 μM). Although the final $S_{gm,l}$ is similar, we can observe that the decrease for tyramine is localized mainly at the lower

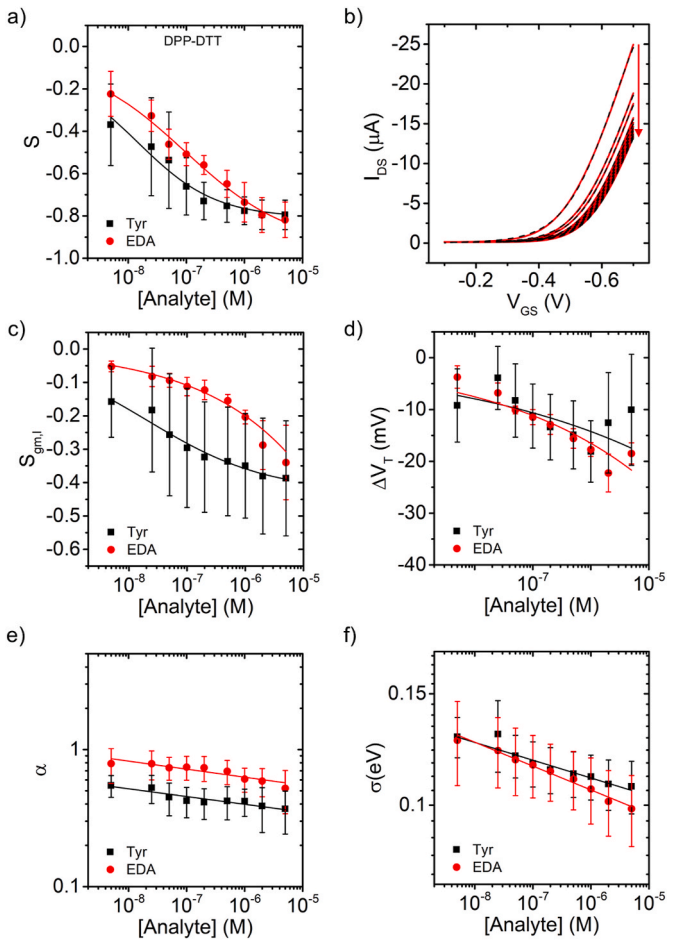

Fig. 5. Analysis of the response of DPP-DTT devices. a) Signal of the current of DPP-DTT devices as a function of biogenic amines concentration. The lines are a guide for the eye of the reader. b) Dashed lines are the best fit obtained using eq 18 in (Zanotti et al., 2024) of the transfer curves reported in Fig. 2a. Best fit parameters as a function of amines concentration: c) $S_{gm,I}$, d) ΔV_t, e) α and f) σ.

concentrations and saturates in μM range, while for EDA the decrease is faster at the higher concentrations and more reproducible (smaller error bars). The ΔV_t trend shown in Fig. 5, is similar for EDA and tyramine, although in the first we observe a monotonic behavior as a function of concentration while in the second the points are more scattered. As observed for PEDOT:PSS, the α parameter is affected by the analyte concentration, decreasing with both amines (Fig. 5e). Also in this case, the energy disorder parameter is not affected by the analyte concentration (Fig. 5f).

The outcome of the analysis underlines how both the linear transconductance (hence dependent on the interfacial capacitance) and the switch-on voltage (hence dependent on the initial doping level) of the device are influenced by the presence of the amines. The device channel parameter σ does not vary with concentration, the band gap being fixed by the reported values for each channel material. The parameter α instead undergoes a smooth variation (−50%) due to the presence of the concentration-sensitive interfacial capacitance. This analysis also shows that the different contributions of the two amines are better resolved for PEDOT:PSS with respect to DPP-DTT, which suggests that the response is correlated with the amines structure and charge, although an extensive study on other amines is necessary to establish selective discrimination. At the same time, the results underline the fact that DPP-DTT devices are in principle able to detect lower amines concentrations compared to PEDOT:PSS EGOTs.

3. Conclusions

We demonstrated an EGOT sensor based on a hydrogel gate made of PEDOT:PSS that can achieve ultrasensitive detection of biogenic amines in solution. Thanks to the different organic semiconducting materials that were used for the channel, it was possible to detect EDA and tyramine across a wide concentration range (nM to mM). The LOD in the order of 100 pM should enable the detection of biogenic amines formed at early food spoilage. The EGOT response embodies both the variation of the charge and the capacitance at the gate/analyte interface. This provides an insight into the electrostatic changes occurring upon recognition, and on the importance of subtle changes at the interface being amplified in the device response. The device architecture that relies on unique patterns for non-covalent interactions can be readily applied to other amines or other molecules able to form electrostatic, hydrogen bonds or p-p stacking interactions with the gate material, which was PEDOT:PSS.

4. Experimental

Reagents. All the reagents and materials were used as provided from the manufacturer without further purifications. Ethylenediamine, tyramine hydrochloride, DMSO, GOPS, $HAuCl_4$, KCl, 1,2-dichlorobenzene and 1X PBS were purchased from Merk-Sigma Aldrich. PEDOT:PSS and DPP-DTT were purchased from Ossila. The Agar powder was purchased from Santa Cruz Biotechnologies.

Materials. The solution for PEDOT:PSS drop casting was prepared by adding 5% m/m dimethylsulfoxide (DMSO) and 0.2% (3-glycidyloxypropyl)trimethoxysilane (GOPS). Formulation for DPP-DTT spin coating was achieved by preparing 5 mg/ml in 1,2-dichlorobenzene.

Data analysis. The response signal $S = \Delta I/I_0$ was measured as the change in the device current normalized by the current in the absence of the analyte (I_0), at a given V_{GS}. The LOD was taken to be the lowest concentration of analyte detectable by the device and was calculated as $LOD = S_{buffer} + 3\sigma$, where S_{buffer} is the signal for PBS in the absence of analyte and σ is the standard deviation.

Electrolyte-Gated Organic Transistors fabrication. The interdigitated (IDE) electrodes on glass (Micrux Technologies) were cleaned in Hellmanex, water and ethanol, by sonicating for 10 min in each solvent. The PEDOT:PSS formulation was diluted 1:1000 with MilliQ H_2O and drop-cast in confined areas of test-patterns (10 μl on a 9.62 mm^2 area) to achieve a PEDOT:PSS semiconductive channel, on IDE with W/L = 49000 (channel length L = 10 μm), and cured in oven at 120 °C for 30 min. DPP-DTT formulation was deposited via spin coating at 2000 rpm (10 μl on a 9.62 mm^2 area) to achieve a DPP-DTT semiconductive channel, on IDE with W/L = 100000 (channel length L = 5 μm), and cured in oven at 140 °C for 30 min. We determined by AFM a thickness of 19 ± 7 nm for PEDOT:PSS films and of 23.7 ± 8.1 nm for DPP-DTT films.

Gate fabrication. Formulation for the PEDOT:PSS hydrogel gate was achieved by pouring 300 μl of a 13% m/m DMSO solution into a polypropylene cup with a diameter of 10 mm and baking it at 75 °C for 3 h. We report in Fig. S2 of Appendix A, a cyclic voltammetry of the gate electrode, showing its mainly capacitive behaviour in buffer.

Agar fabrication. Formulation for the agar hydrogel electrolyte was prepared by pouring 1X PBS of a 2% m/v Agar solution into a vial and baking it at 90 °C for 30 min, it subsequently left to solidify in a petri dish from which cylinders are obtained.

Electrical Characterization. The transfer curves were measured at room temperature inside a Faraday cage by means of an Agilent (B2902A) Source Measure Unit (SMU) by fixing the V_{DS} at −0.1 V and sweeping the gate source voltage between −0.2 V and 0.6 V (for devices based on PEDOT:PSS) and between −0.1 V and −0.7 V (for devices based on DPP-DTT). The electrolyte consisted of a 50 μl drop of PBS (phosphate buffered saline, pH 7.4) containing increasing concentrations of Tyramine or Ethylenediamine, ranging from 5 nM to 5 mM,

under static conditions. The analyte solution was confined in the PEDOT:PSS gate and replaced for each concentration.

Electrochemical deposition. A potenziostat/galvanostat CH instrument model 760 was used for gold electrochemical deposition. The gate was connected as working electrode, with a platinum wire connected as both counter and reference electrode. The deposition was performed in 0.1 M KCl and 5 mM $HAuCl_4$ at 0.1 Vs^{-1} applying a potential between 0.5 V and −0.5 V for ten cycles.

CRediT authorship contribution statement

Ilenia Sergi: Writing – original draft, Investigation, Data curation. **Matteo Sensi:** Writing – review & editing, Writing – original draft, Visualization, Supervision, Formal analysis, Data curation, Conceptualization. **Rian Zanotti:** Writing – review & editing, Investigation. **Theofania Tsironi:** Writing – original draft. **Emmanouil Flemetakis:** Writing – original draft, Funding acquisition. **Deborah Mary Power:** Writing – original draft, Funding acquisition. **Carlo Augusto Bortolotti:** Writing – review & editing, Writing – original draft, Funding acquisition. **Fabio Biscarini:** Writing – review & editing, Writing – original draft, Supervision, Funding acquisition, Conceptualization.

Declaration of competing interest

The authors declare that they have no known competing financial interests or personal relationships that could have appeared to influence the work reported in this paper.

Acknowledgements

This paper is supported by the PRIMA program under grant agreement No 1468, project FRUALGAE. The PRIMA program is supported by the European Union. This Project received funding from the European Union's Horizon 2020 research and innovation programme under the Marie Sklodowska-Curie Grant agreement 872217 (Project ICHTHYS). The publication was supported by co-financing from the European Union - FSE-REACT-EU, PON research and Innovation 2014–2020 DM1062/2021.

Appendix A. Supplementary data

Supplementary data to this article can be found online at https://doi.org/10.1016/j.bios.2024.117098.

Data availability

Data will be made available on request.

References

Arthur, J.N., Burns, S., Cole, C.M., Barthelme, Q.T., Yambem, S.D., 2022. PEDOT:PSS hydrogel gate electrodes for OTFT sensors. J. Mater. Chem C 10, 13964–13973. https://doi.org/10.1039/d2tc01096h.

Arulkumar, A., Paramithiotis, S., Paramasivam, S., 2023. Biogenic amines in fresh fish and fishery products and emerging control. Aquac Fish 8, 431–450. https://doi.org/10.1016/j.aaf.2021.02.001.

Bachrach, U., 2005. Naturally occurring polyamines: interaction with macromolecules. Curr. Protein Pept. Sci. 6, 559–566. https://doi.org/10.2174/138920305774933240.

Berto, M., Casalini, S., Di Lauro, M., Marasso, S.L., Cocuzza, M., Perrone, D., Pinti, M., Cossarizza, A., Pirri, C.F., Simon, D.T., Berggren, M., Zerbetto, F., Bortolotti, C.A., Biscarini, F., 2016. Biorecognition in organic field effect transistors biosensors: the role of the density of states of the organic semiconductor. Anal. Chem. 88, 12330–12338. https://doi.org/10.1021/acs.analchem.6b03522.

Berto, M., Diacci, C., D'Agata, R., Pinti, M., Bianchini, E., Lauro, M. Di, Casalini, S., Cossarizza, A., Berggren, M., Simon, D., Spoto, G., Biscarini, F., Bortolotti, C.A., 2018. EGOFET peptide aptasensor for label-free detection of inflammatory cytokines in complex fluids. Adv. Biosyst. 2. https://doi.org/10.1002/adbi.201700072.

Bihar, E., Deng, Y., Miyake, T., Saadaoui, M., Malliaras, G.G., Rolandi, M., 2016. A Disposable paper breathalyzer with an alcohol sensing organic electrochemical transistor. Sci. Rep. 6, 2–7. https://doi.org/10.1038/srep27582.

Biji, K.B., Ravishankar, C.N., Venkateswarlu, R., Mohan, C.O., Gopal, T.K.S., 2016. Biogenic amines in seafood: a review. J. Food Sci. Technol. https://doi.org/10.1007/s13197-016-2224-x.

Burtscher, B., Manco Urbina, P.A., Diacci, C., Borghi, S., Pinti, M., Cossarizza, A., Salvarani, C., Berggren, M., Biscarini, F., Simon, D.T., Bortolotti, C.A., 2021. Sensing inflammation biomarkers with electrolyte-gated organic electronic transistors. Adv. Healthcare Mater. https://doi.org/10.1002/adhm.202100955.

Casalini, S., Dumitru, A.C., Leonardi, F., Bortolotti, C.A., Herruzo, E.T., Campana, A., De Oliveira, R.F., Cramer, T., Garcia, R., Biscarini, F., 2015. Multiscale sensing of antibody-antigen interactions by organic transistors and single-molecule force spectroscopy. ACS Nano 9, 5051–5062. https://doi.org/10.1021/acsnano.5b00136.

Chennit, K., Delavari, N., Mekhmoukhen, S., Boukraa, R., Fillaud, L., Zrig, S., Battaglini, N., Piro, B., Noël, V., Zozoulenko, I., Mattana, G., 2023. Inkjet-Printed, coplanar electrolyte-gated organic field-effect transistors on flexible substrates: fabrication, modeling, and applications in biodetection. Adv. Mater. Technol. 8. https://doi.org/10.1002/admt.202200300.

Doeun, D., Davaatseren, M., Chung, M.S., 2017. Biogenic amines in foods. Food Sci. Biotechnol. https://doi.org/10.1007/s10068-017-0239-3.

Erim, F.B., 2013. Recent analytical approaches to the analysis of biogenic amines in food samples. TrAC, Trends Anal. Chem. https://doi.org/10.1016/j.trac.2013.05.018.

Galliani, M., Diacci, C., Berto, M., Sensi, M., Beni, V., Berggren, M., Borsari, M., Simon, D. T., Biscarini, F., Bortolotti, C.A., 2020. Flexible printed organic electrochemical transistors for the detection of uric acid in artificial wound exudate. Adv. Mater. Interfac. 7. https://doi.org/10.1002/admi.202001218.

Gentile, F., Vurro, F., Janni, M., Manfredi, R., Cellini, F., Petrozza, A., Zappettini, A., Coppedè, N., 2022. A biomimetic, biocompatible OECT sensor for the real-time measurement of concentration and saturation of ions in plant sap. Adv. Electron. Mater. 8. https://doi.org/10.1002/aelm.202200092.

Gentili, D., D'Angelo, P., Militano, F., Mazzei, R., Poerio, T., Brucale, M., Tarabella, G., Bonetti, S., Marasso, S.L.L., Cocuzza, M., Giorno, L., Iannotta, S., Cavallini, M., 2018. Integration of organic electrochemical transistors and immuno-affinity membranes for label-free detection of interleukin-6 at the physiological concentration range through antibody-antigen recognition. J. Mater. Chem. B 2–3. https://doi.org/10.1039/C8TB01697F.

Giordani, M., Sensi, M., Berto, M., Di Lauro, M., Bortolotti, C.A., Gomes, H.L., Zoli, M., Zerbetto, F., Fadiga, L., Biscarini, F., 2020. Neuromorphic organic devices that specifically discriminate dopamine from its metabolites by nonspecific interactions. Adv. Funct. Mater. 30. https://doi.org/10.1002/adfm.202002141.

Givanoudi, S., Heyndrickx, M., Depuydt, T., Khorshid, M., Robbens, J., Wagner, P., 2023. A review on bio- and chemosensors for the detection of biogenic amines in food safety applications: the status in 2022. Sensors. https://doi.org/10.3390/s23020613.

Gualandi, I., Tessarolo, M., Mariani, F., Arcangeli, D., Possanzini, L., Tonelli, D., Fraboni, B., Scavetta, E., 2020. Layered double hydroxide-modified organic electrochemical transistor for glucose and lactate biosensing. Sensors 20, 1–15. https://doi.org/10.3390/s20123453.

Gualandi, I., Tonelli, D., Mariani, F., Scavetta, E., Marzocchi, M., Fraboni, B., 2016. Selective detection of dopamine with an all PEDOT:PSS organic electrochemical transistor. Sci. Rep. 6. https://doi.org/10.1038/srep35419.

Guo, K., Wustoni, S., Koklu, A., Díaz-Galicia, E., Moser, M., Hama, A., Alqahtani, A.A., Ahmad, A.N., Alhamlan, F.S., Shuaib, M., Pain, A., McCulloch, I., Arold, S.T., Grünberg, R., Inal, S., 2021. Rapid single-molecule detection of COVID-19 and MERS antigens via nanobody-functionalized organic electrochemical transistors. Nat. Biomed. Eng. 5, 666–677. https://doi.org/10.1038/s41551-021-00734-9.

Hsieh, C.H., Huang, C.H., Chu, P.L., Chu, S.Y., Chen, P., 2021. Investigation of the mechanism of a facile method for ammonia treatment to effectively tune the morphology and conductivity of PEDOT:PSS films. Org. Electron. 91, 106081. https://doi.org/10.1016/j.orgel.2021.106081.

Jia, H., Huang, Z., Li, P., Zhang, S., Wang, Y., Wang, J.-Y., Gu, X., Lei, T., 2021. Engineering donor–acceptor conjugated polymers for high-performance and fast-response organic electrochemical transistors. J Mater Chem C 9, 4927–4934. https://doi.org/10.1039/D1TC00440A.

Jing, W., Xu, X., Yu, L., Peng, Q., 2023. Structure influence of amine-containing additives on the solution state and out-of-plane conductivity of PEDOT:PSS for efficient organic solar cells. Macromol. Rapid Commun. 44. https://doi.org/10.1002/marc.202300400.

Keene, S.T., van der Pol, T.P.A., Zakhidov, D., Weijtens, C.H.L., Janssen, R.A.J., Salleo, A., van de Burgt, Y., 2020. Enhancement-mode PEDOT:PSS organic electrochemical transistors using molecular de-doping. Adv. Mater. 32. https://doi.org/10.1002/adma.202000270.

Kergoat, L., Piro, B., Berggren, M., Pham, M., Yassar, A., 2012. DNA detection with a water-gated organic field-effect transistor. Org. Electron. 13, 1–6. https://doi.org/10.1016/j.orgel.2011.09.025.

Kumar, P., Yi, Z., Zhang, S., Sekar, A., Soavi, F., Cicoira, F., 2015. Effect of channel thickness, electrolyte ions, and dissolved oxygen on the performance of organic electrochemical transistors. Appl. Phys. Lett. 107. https://doi.org/10.1063/1.4927595.

Lai, S., Viola, F.A., Cosseddu, P., Bonfiglio, A., 2018. Floating gate, organic field-effect transistor-based sensors towards biomedical applications fabricated with large-area processes over flexible substrates. Sensors 18. https://doi.org/10.3390/s18030688.

Li, B., Lu, S., 2020. The importance of amine-degrading enzymes on the biogenic amine degradation in fermented foods: a review. Process Biochem. https://doi.org/10.1016/j.procbio.2020.09.012.

Li, S., Zhong, T., Long, Q., Huang, C., Chen, L., Lu, D., Li, X., Zhang, Z., Shen, G., Hou, X., 2021. A gold nanoparticles-based molecularly imprinted electrochemical sensor for

histamine specific-recognition and determination. Microchem. J. 171. https://doi.org/10.1016/j.microc.2021.106844.
Macchia, E., Manoli, K., Holzer, B., Di Franco, C., Ghittorelli, M., Torricelli, F., Alberga, D., Mangiatordi, G.F., Palazzo, G., Scamarcio, G., Torsi, L., 2018. Single-molecule detection with a millimetre-sized transistor. Nat. Commun. 9. https://doi.org/10.1038/s41467-018-05235-z.
Magliulo, M., De Tullio, D., Vikholm-Lundin, I., Albers, W.M., Munter, T., Manoli, K., Palazzo, G., Torsi, L., 2016. Label-free C-reactive protein electronic detection with an electrolyte-gated organic field-effect transistor-based immunosensor. Anal. Bioanal. Chem. 408, 3943–3952. https://doi.org/10.1007/s00216-016-9502-3.
Marutaphan, A., Seekaew, Y., Wongchoosuk, C., 2017. Self-consistent charge density functional tight-binding study of poly(3,4-ethylenedioxythiophene): poly (styrenesulfonate) ammonia gas sensor. Nanoscale Res. Lett. 12. https://doi.org/10.1186/s11671-017-1878-2.
Minami, T., Sato, T., Minamiki, T., Tokito, S., 2015. An extended-gate type organic FET based biosensor for detecting biogenic amines in aqueous solution. Anal. Sci. 31, 721–724. https://doi.org/10.2116/analsci.31.721.
Minamiki, T., Hashima, Y., Sasaki, Y., Minami, T., 2018. An electrolyte-gated polythiophene transistor for the detection of biogenic amines in water. Chem. Commun. 54, 6907–6910. https://doi.org/10.1039/c8cc02462f.
Nerín, C., Aznar, M., Carrizo, D., 2016. Food contamination during food process. Trends Food Sci. Technol. https://doi.org/10.1016/j.tifs.2015.12.004.
Omer, A.K., Mohammed, R.R., Mohammed Ameen, P.S., Abas, Z.A., Ekici, K., 2021. Presence of biogenic amines in food and their public health implications: a review. J. Food Protect. https://doi.org/10.4315/JFP-21-047.
Önal, A., 2007. A review: current analytical methods for the determination of biogenic amines in foods. Food Chem. 103, 1475–1486. https://doi.org/10.1016/j.foodchem.2006.08.028.
Pallu, J., Avci-Adali, M., Mackeben, P., Mohammadnejad, L., Mattana, G., Noël, V., Piro, B., 2019. A DNA hydrogel gated organic field effect transistor. Org. Electron. 75. https://doi.org/10.1016/j.orgel.2019.105402.
Pappa, A.M., Ohayon, D., Giovannitti, A., Maria, I.P., Savva, A., Uguz, I., Rivnay, J., McCulloch, I., Owens, R.M., Inal, S., 2018. Direct metabolite detection with an n-type accumulation mode organic electrochemical transistor. Sci. Adv. 4, 1–8. https://doi.org/10.1126/sciadv.aat0911.
Rivnay, J., Inal, S., Salleo, A., Owens, R.M., Berggren, M., Malliaras, G.G., 2018. Organic electrochemical transistors. Nat. Rev. Mater. 3. https://doi.org/10.1038/natrevmats.2017.86.
Ruiz-Capillas, C., Herrero, A.M., 2019. Impact of biogenic amines on food quality and safety. Foods. https://doi.org/10.3390/foods8020062.
Sensi, M., Berto, M., Gentile, S., Pinti, M., Conti, A., Pellacani, G., Salvarani, C., Cossarizza, A., Bortolotti, C.A., Biscarini, F., 2021. Anti-drug antibody detection with label-free electrolyte-gated organic field-effect transistors. Chem. Commun. 57, 367–370. https://doi.org/10.1039/d0cc03399e.
Sensi, M., de Oliveira, R.F., Berto, M., Palmieri, M., Ruini, E., Livio, P.A., Conti, A., Pinti, M., Salvarani, C., Cossarizza, A., Cabot, J.M., Ricart, J., Casalini, S., González-García, M.B., Fanjul-Bolado, P., Bortolotti, C.A., Samorì, P., Biscarini, F., 2023. Reduced graphene oxide electrolyte-gated transistor immunosensor with highly selective multiparametric detection of anti-drug antibodies. Adv. Mater. 35. https://doi.org/10.1002/adma.202211352.
Sensi, M., Migatti, G., Beni, V., D'Alvise, T.M., Weil, T., Berto, M., Greco, P., Imbriano, C., Biscarini, F., Bortolotti, C.A., 2022. Monitoring DNA hybridization with organic electrochemical transistors functionalized with polydopamine. Macromol. Mater. Eng. 307, 2100880. https://doi.org/10.1002/mame.202100880.
Sensi, M., Ricci, A., Rigillo, G., Paradisi, A., Berto, M., Gnesutta, N., Imbriano, C., Biscarini, F., Bortolotti, C.A., 2024. Investigation of transcription factor–DNA binding with electrolyte-gated organic transistors. J Mater Chem C. https://doi.org/10.1039/d4tc00260a.
Song, Q., Wang, W., Liang, J., Chen, C., Cao, Y., Cai, B., Chen, B., He, R., 2023. Fabrication of PEDOT:PSS-based solution gated organic electrochemical transistor array for cancer cells detection. RSC Adv. 13, 36416–36423. https://doi.org/10.1039/d3ra06800e.
Strakosas, X., Bongo, M., Owens, R.M., 2015. The organic electrochemical transistor for biological applications. J. Appl. Polym. Sci. 132, 1–14. https://doi.org/10.1002/app.41735.
Torre, R., Costa-Rama, E., Nouws, H.P.A., Delerue-Matos, C., 2020. Screen-printed electrode-based sensors for food spoilage control: bacteria and biogenic amines detection. Biosensors. https://doi.org/10.3390/BIOS10100139.
Torricelli, F., Adrahtas, D.Z., Bao, Z., Berggren, M., Biscarini, F., Bonfiglio, A., Bortolotti, C.A., Frisbie, C.D., Macchia, E., Malliaras, G.G., McCulloch, I., Moser, M., Nguyen, T.-Q., Owens, R.M., Salleo, A., Spanu, A., Torsi, L., 2021. Electrolyte-gated transistors for enhanced performance bioelectronics. Nature Rev. Methods Primers 1, 66. https://doi.org/10.1038/s43586-021-00065-8.
Van Der Pol, T.P.A., Keene, S.T., Saes, B.W.H., Meskers, S.C.J., Salleo, A., Van De Burgt, Y., Janssen, R.A.J., 2019. The mechanism of dedoping PEDOT:PSS by aliphatic polyamines. J. Phys. Chem. C 123, 24328–24337. https://doi.org/10.1021/acs.jpcc.9b07718.
Vasconcelos, H., Coelho, L.C.C., Matias, A., Saraiva, C., Jorge, P.A.S., de Almeida, J.M.M. M., 2021. Biosensors for biogenic amines: a review. Biosensors. https://doi.org/10.3390/bios11030082.
Verma, N., Hooda, Vinita, Gahlaut, A., Gothwal, A., Hooda, Vikas, 2020. Enzymatic biosensors for the quantification of biogenic amines: a literature update. Crit. Rev. Biotechnol. https://doi.org/10.1080/07388551.2019.1680600.
Wang, L., Wu, Z., Cao, C., 2019. Technologies and fabrication of intelligent packaging for perishable products. Appl. Sci. 9. https://doi.org/10.3390/app9224858.
White, S.P., Dorfman, K.D., Frisbie, C.D., 2016. Operating and sensing mechanism of electrolyte-gated transistors with floating gates: building a platform for amplified biodetection. J. Phys. Chem. C 120, 108–117. https://doi.org/10.1021/acs.jpcc.5b10694.
Zanotti, R., Sensi, M., Berto, M., Paradisi, A., Bianchi, M., Greco, P., Bortolotti, C.A., Di Lauro, M., Biscarini, F., 2024. Charge carrier density in organic semiconductors modulates the effective capacitance: a unified view of electrolyte gated organic transistors. Adv. Mater. https://doi.org/10.1002/adma.202410940.